

# Broadening of the second-harmonic phase-matching bandwidth in type II periodically poled KTP

Rui Wu, Yuping Chen, Junfeng Zhang, Xianfeng Chen, and Yuxing Xia

We have theoretically demonstrated type II broadband second-harmonic generation (SHG) based on a quasi-phase-matching (QPM) configuration in periodically poled KTP (PPKTP). The wavelength dependence of QPM grating periods at different temperatures of 5 °C, 25 °C, and 45 °C is calculated with the crystal length of 1 cm. We find a very wide bandwidth, as large as 42.6 nm, of fundamental wavelength of 1.58  $\mu\text{m}$  at the telecommunication band with the QPM period of 48.9  $\mu\text{m}$  at 25 °C. The corresponding bandwidths of incident angle and temperature are found to be 4.24° and 14.8 °C, respectively. The comparison among PPKTP, periodically poled lithium niobate (PPLN), and MgO:PPLN reveals the unique performance of PPKTP in the broadband SHG. © 2005 Optical Society of America

OCIS codes: 190.2620, 190.4400.

## 1. Introduction

In recent years, applications of quasi-phase-matching (QPM) nonlinear optical frequency conversion with different periodically poled crystals have been growing rapidly. High-efficiency QPM second-harmonic generation (SHG) is achieved by periodic reversal of the sign of the nonlinear coefficient to compensate the phase velocity mismatch between the fundamental and the second-harmonic (SH) waves. To obtain the wide QPM wavelength bandwidth for quadratic nonlinear optical interaction, periodically poled MgO-doped lithium niobate (MgO:PPLN) has been investigated with a type I QPM configuration.<sup>1</sup> Although a bandwidth as large as 52 nm can be expected at the communication band, the efficiency of the broadband SHG in MgO:PPLN is sensitive to the sample temperature (the acceptance bandwidth of temperature is only  $\sim 1.3$  °C),<sup>1,2</sup> which is inconvenient to maintain pulsed energy stability of the converted beam.

Periodically poled KTP (PPKTP) has been attracting considerable interest for SHG due to its high nonlinearity, low susceptibility to photorefractive

damage, relatively high damage threshold, and good power-handling capability.<sup>3</sup> PPKTP can be fabricated more easily than PPLN or lithium tantalate by means of electric field poling because of its lower coercive field and quasi-one-dimensional structure.<sup>3</sup> Up to now, research has focused mostly on the type I QPM nonlinear optical process. For type II QPM in PPKTP, the domain-inversion SHG grating period is larger than that for type I QPM, making it easier to obtain homogeneous poling over large product volumes.<sup>4</sup> Furthermore, type II QPM has the advantages of a larger phase-matching bandwidth and easier separation of the SH and the fundamental waves, which is desirable for frequency-doubling arrangements.<sup>4</sup> To the best of our knowledge, the properties of first-order type II SHG by QPM in PPKTP at the telecommunication band has been scarcely investigated, although some studies about its effect and role in the visible or mid-infrared region are available in the literature.<sup>3-9</sup>

In this paper we discuss the broadband properties of first-order type II QPM SHG in PPKTP at the telecommunication band. The wavelength dependence of the QPM grating period and the bandwidths of fundamental wavelength, temperature, and incident angle are numerically calculated and explained. Furthermore, we compare the type II broadband SHG in PPKTP with other crystals, i.e., MgO:PPLN and PPLN, in detail.

## 2. Numerical Calculations and Discussion

First-order type II QPM SHG in PPKTP is realized by use of the  $d_{24}$  nonlinear coefficient for a Z-cut crystal with the beam propagation along the  $x$  axis. It can be

---

The authors are with the Institute of Optics and Photonics, Department of Physics, State Key Laboratory on Fiber Optic Local Area Communication Networks and Advanced Optical Communication Systems, Shanghai Jiao Tong University, 800 Dongchuan Road, Shanghai 200240, People's Republic of China. The e-mail address for Y. Chen is ypchen@sjtu.edu.cn.

Received 4 October 2004; revised manuscript received 26 January 2005; accepted 10 February 2005.

0003-6935/05/265561-04\$15.00/0

© 2005 Optical Society of America

expressed as  $E_y^\omega E_z^\omega \rightarrow E_y^{2\omega}$ , where  $E_i^\omega (i = x, y, z)$  is the electric field component at a frequency  $\omega$ , parallel to the  $i$  axis of the crystal.

With a small-signal approximation, the normalized SH intensity  $\eta$  of QPM can be described as

$$\eta \propto \text{sinc}^2(\Delta k_{24}L/2), \quad (1)$$

where  $L$  is the crystal length.  $\Delta k_{24}$  is the overall phase mismatch between interactive light waves and QPM gratings,

$$\begin{aligned} \Delta k_{24} &= k_{2y} - k_{1y} - k_{1z} - \frac{2\pi}{\Lambda_1} \\ &= \frac{2\pi(2n_{2y} - n_{1y} - n_{1z})}{\lambda} - \frac{2\pi}{\Lambda_1}, \end{aligned} \quad (2)$$

where  $\Lambda_1$  is the first-order QPM grating period of frequency doubling in the type II QPM case.

When the QPM grating period<sup>3</sup>

$$\Lambda_1 = \frac{2\pi}{\Delta k_{24}'} \lambda / (2n_{2y} - n_{1y} - n_{1z}) \quad (3)$$

is satisfied, where  $\Delta k_{24}' = k_{2y} - k_{1y} - k_{1z}$  is the wave-vector mismatch, the type II SHG in PPKTP is phase matched.

For first-order type II QPM SHG of a broadband optical wave, the dependence of the wave-vector mismatch on wavelength can be derived as

$$\frac{d(\Delta k_{24}')}{d\lambda} = \frac{2\pi c}{\lambda^2} \delta, \quad (4)$$

where  $\delta = 1/v_{g_{1y}} + 1/v_{g_{1z}} - 2/v_{g_{2y}}$  is the group-velocity walk-off parameter, with  $v_{g_{1i}}$  and  $v_{g_{2i}}$  being the group velocities for the fundamental (subscript 1) and the harmonic (subscript 2). If a certain local extremum  $d(\Delta k_{24}')/d\lambda = 0$  of the unique dispersion can be achieved in the spectral region, the group-velocity matching (GVM) ( $\delta = 0$ ) can be obtained correspondingly.<sup>1</sup> Therefore the GVM and broadband QPM SHG are satisfied simultaneously.

#### A. Broadband Second-Harmonic Generation Grating Period and Wavelength Tuning Rate on Temperature

Figure 1 shows how the QPM grating period varies with the fundamental wavelength for type II SHG in PPKTP from 1.50 to 1.65  $\mu\text{m}$  at three different temperatures of 5  $^\circ\text{C}$ , 25  $^\circ\text{C}$ , and 45  $^\circ\text{C}$ . We set the length of the PPKTP to 1 cm. (For general purposes, the length of the PPKTP is supposed to be 1 cm in the following simulations.) The grating period  $\Lambda$  is calculated according to the Sellmeier equations of KTP with the thermal-optic coefficients at 25  $^\circ\text{C}$  from CASIX.<sup>10</sup>

From Fig. 1, the grating period of the type II SHG in PPKTP reaches the maximum value around the telecommunication wavelength (we call it the broad-

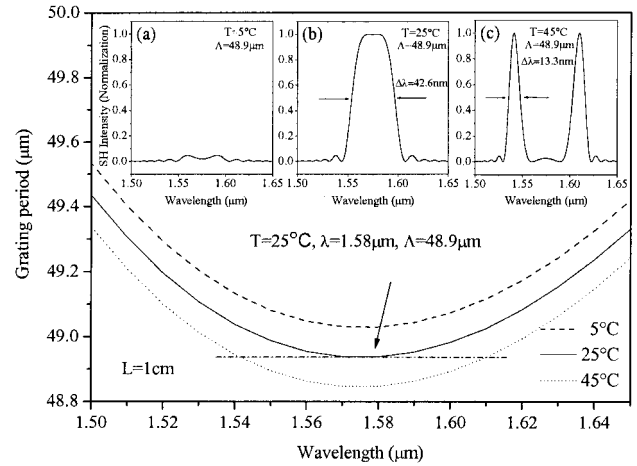


Fig. 1. Period of QPM gratings as a function of the fundamental wavelength at three different temperatures of 5  $^\circ\text{C}$ , 25  $^\circ\text{C}$ , and 45  $^\circ\text{C}$ . The maximum grating period  $\Lambda$  is 48.9  $\mu\text{m}$  at the broadband SHG center wavelength of 1.58  $\mu\text{m}$  at 25  $^\circ\text{C}$ . The insets are the normalized SH intensity versus the fundamental wavelength at the corresponding temperatures with the grating period of 48.9  $\mu\text{m}$ , respectively.

band SHG center wavelength hereinafter), where the broad bandwidth can be expected. We draw a tangent line on the curve at the temperature of 25  $^\circ\text{C}$  and find that the grating period is 48.9  $\mu\text{m}$  and the fundamental wavelength is 1.58  $\mu\text{m}$ . A broadband of 42.6 nm can be obtained at 1.58  $\mu\text{m}$ , as displayed in inset (b) of Fig. 1. The variation in temperature will shift the curve of the grating period up or down. For instance, when the QPM grating period of 48.9  $\mu\text{m}$  is fixed, the tangent line would intersect two cross points with the curve at the temperature of 45  $^\circ\text{C}$ , where only the QPM condition can be satisfied and broadband SHG cannot be achieved. At the two cross points, we can obtain two QPM SHG peaks with the same bandwidth of  $\sim 13.3$  nm as shown in inset (c) of Fig. 1. However, once the temperature is lower than 25  $^\circ\text{C}$ , the horizontal line does not have a cross point with the downward curve (the dashed curve is drawn at 5  $^\circ\text{C}$  as an example). Without satisfying both GVM and QPM, no QPM peak is expected and the SH intensity is very low, as shown in inset (a) of Fig. 1, and the maximum value of the normalized intensity of the SHG is only  $\sim 0.046$  at 5  $^\circ\text{C}$ .

It is interesting to note that the two cross points between the curve and the horizontal line shift to the visible and near-infrared regions, respectively, with the increase in temperature [see inset (c) of Fig. 1]. For example, we calculate the normalized SH intensity versus the fundamental wavelength in the temperature range from 45  $^\circ\text{C}$  to 180  $^\circ\text{C}$  (not shown in Fig. 1). The two positions of maximum normalized SH intensity at 45  $^\circ\text{C}$  are centered at 1544 and 1611 nm. While at the temperature of 180  $^\circ\text{C}$ , the two peak intensities transfer to 1484 and 1675 nm with the same bandwidth of 4 nm. For type II SHG with two maximum normalized SH intensities in PPKTP, the wavelength tuning rate on temperature  $d\lambda/dT$  can

thus be evaluated as  $0.5 \text{ nm}/^\circ\text{C}$  from  $45^\circ\text{C}$  to  $180^\circ\text{C}$ . Therefore we could obtain the tunable SH output toward the visible and near-infrared regions by changing the temperature.

### B. Wavelength Bandwidth

We calculated the FWHM (full width at half-maximum) of the normalized SH intensity  $\eta$  at each of the broadband SHG center wavelengths from  $1.52$  to  $1.68 \mu\text{m}$ , and the results of the wavelength bandwidth of QPM SHG in PPKTP are shown in Fig. 2. There is a relative minimum wavelength bandwidth at  $\sim 42.6 \text{ nm}$  at  $1.58 \mu\text{m}$ , as displayed in inset (b) of Fig. 2. However, the bandwidth around  $1.58 \mu\text{m}$  is larger than  $42.6 \text{ nm}$ , which is apparently inconsistent with the discussion in Fig. 1. The reason is closely related to the interval between the two cross points intersected by the horizontal line in Fig. 1. If the interval between the two points is near enough, the SH intensities at the two corresponding wavelengths would overlap to a wider broadband, which is larger than the bandwidth at the broadband SHG center wavelength. However, a disadvantage of the wider bandwidth mentioned above is that significant ripples are always present within the passband. The insets in Fig. 2 are the wavelength dependence of the normalized SH intensity at  $1.56$  and  $1.58 \mu\text{m}$ , respectively. The grating period is  $48.9 \mu\text{m}$  and the temperature is  $25^\circ\text{C}$ . It can be seen from inset (a) of Fig. 2 that the SH intensities at  $1.56$  and  $1.60 \mu\text{m}$  are overlapped. The bandwidth at  $1.56 \mu\text{m}$  is as large as  $51.7 \text{ nm}$ . Once the interval between the two cross points is larger, the two SH intensities would not overlap any more. Then the wavelength bandwidth would become rapidly narrower with wavelength apart from the broadband SHG center wavelength.

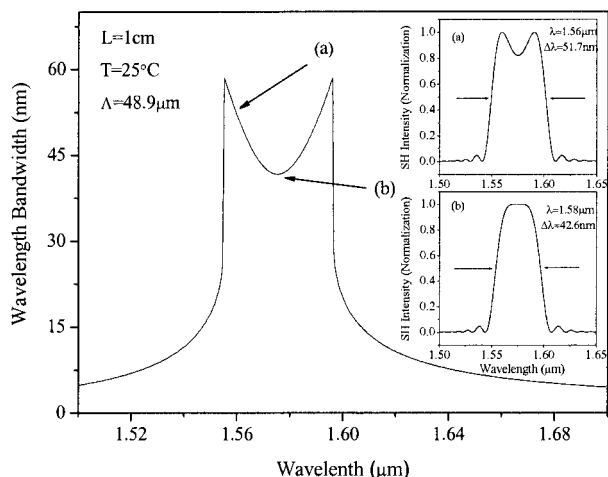


Fig. 2. Wavelength bandwidth of QPM SHG versus fundamental wavelength at  $25^\circ\text{C}$ . The insets are the wavelength dependence of the normalized SH intensity at the center wavelength of  $1.56$  and  $1.58 \mu\text{m}$  under the grating period of  $48.9 \mu\text{m}$ , respectively.

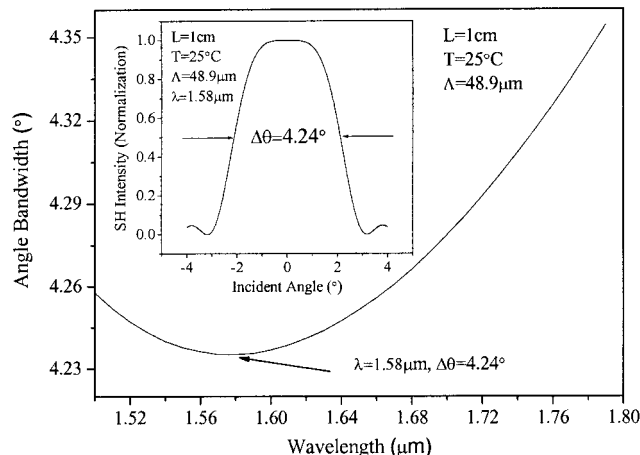


Fig. 3. Incident angle bandwidth versus fundamental wavelength at  $25^\circ\text{C}$ . The normalized SH intensity as a function of the incident angle at  $1.58 \mu\text{m}$  is shown in the inset and the angle bandwidth  $\Delta\theta$  is  $4.24^\circ$ .

### C. Angle Bandwidth and Temperature Bandwidth

Similarly, according to the grating period  $\Lambda$  required for the first-order QPM at an angle  $\theta$ ,<sup>11</sup> we also calculate the incident angle bandwidth versus the fundamental wavelength at  $25^\circ\text{C}$  under the grating period of  $48.9 \mu\text{m}$  in the wavelength range from  $1.50$  to  $1.80 \mu\text{m}$ , as shown in Fig. 3. Compared with the spectral region without broadband SHG, the generation of broadband SHG limits the angle variation, which results in the minimum angle bandwidth  $\Delta\theta = 4.24^\circ$  at  $1.58 \mu\text{m}$ , as shown in the inset of Fig. 3.

By the aid of the Sellmeier equations of KTP with the thermal-optic coefficients at  $25^\circ\text{C}$  from CASIX,<sup>10</sup> the SH intensity versus temperature at the wavelength of  $1.58 \mu\text{m}$  is displayed in Fig. 4. The temperature bandwidth  $\Delta T$  is  $\sim 14.8^\circ\text{C}$  at this broadband SHG center wavelength with a grating period of  $48.9 \mu\text{m}$ . We find that the temperature bandwidth is rather large. The wide temperature bandwidth of the type II SHG in PPKTP is highly advantageous to

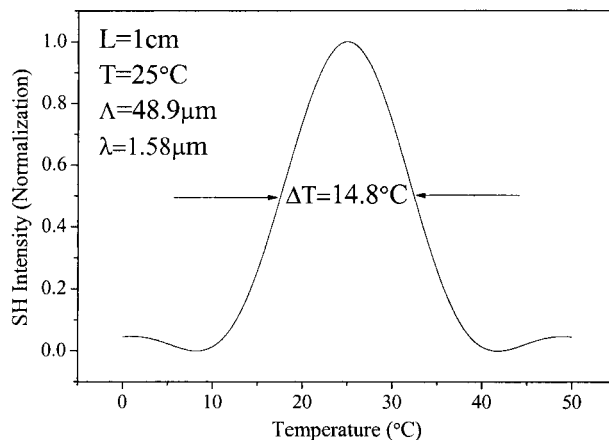


Fig. 4. Normalized SH intensity versus temperature at  $1.58 \mu\text{m}$ . The temperature bandwidth  $\Delta T$  is  $\sim 14.8^\circ\text{C}$ .

Table 1. Comparison of Broadband QPM SHG in PPKTP ( $E_y^\omega E_z^\omega \rightarrow E_y^{2\omega}$ ), MgO:PPLN ( $o + o \rightarrow e$ ), and PPLN ( $o + o \rightarrow e$ )<sup>a</sup>

Crystal	Nonlinear Coefficient (pm/V)	Coercive Field (kV/mm)	Grating Period ( $\mu\text{m}$ )	Center Wavelength ( $\mu\text{m}$ )	Wavelength Bandwidth (nm)	Temperature Bandwidth ( $^\circ\text{C}$ )	Incident Angle Bandwidth ( $^\circ$ )
PPKTP ( $E_y^\omega E_z^\omega \rightarrow E_y^{2\omega}$ )	$d_{24} = 3.64^b$	$2^b$	48.9	1.58	42.6	14.8	4.24
MgO:PPLN ( $o + o \rightarrow e$ )	$d_{31} = 3.4^c$	$4.5^b$	23.4	1.55	30.1	0.22	2.93
PPLN ( $o + o \rightarrow e$ )	$d_{31} = 5.95^d$	$21^b$	23.8	1.61	32.6	0.56	3.56

<sup>a</sup>Crystal length  $L = 1$  cm and temperature  $T = 25$   $^\circ\text{C}$ .

<sup>b</sup>Ref. 12.

<sup>c</sup>Ref. 1.

<sup>d</sup>Ref. 10.

maintain pulsed energy stability of the converted beam in the application of frequency conversion.<sup>5</sup>

### D. Discussion and Comparison

Since the local extremum  $d(\Delta k_{24}')/d\lambda = 0$  cannot be achieved in the spectral region, broadband SHG does not occur for type I SHG in PPKTP. The comparison of the three crystals, PPKTP ( $E_y^\omega E_z^\omega \rightarrow E_y^{2\omega}$ ), MgO:PPLN ( $o + o \rightarrow e$ ), and PPLN ( $o + o \rightarrow e$ ), using broadband QPM SHG is summarized in Table 1.

From Table 1 we can see that the broadband SHG in PPLN ( $o + o \rightarrow e$ ) is not at the telecommunication band, which is also one of the reasons why people choose other crystals, e.g., MgO:PPLN and PPKTP, as substitutes. Compared with those of MgO:PPLN ( $o + o \rightarrow e$ ), the grating period, as well as the bandwidths of fundamental wavelength, temperature, and incident angle, are all larger in PPKTP. Since the coercive field of PPKTP is lowest in the three crystals, it is more easily fabricated by means of electric field poling. On the basis of the above reasons, PPKTP is believed to be more favorable for broadband SHG at the telecommunication band using type II QPM SHG than MgO:PPLN and PPLN with the same process of  $o + o \rightarrow e$ .

### 3. Conclusion

In summary, we have theoretically demonstrated type II broadband SHG in PPKTP at the telecommunication band. The dependence of the wave-vector mismatch on wavelength is analyzed to achieve broadband SHG in the type II case. A bandwidth of 42.6 nm at the wavelength of 1.58  $\mu\text{m}$  at 25  $^\circ\text{C}$  is obtained with the crystal length of 1 cm under the grating period of 48.9  $\mu\text{m}$ . Temperature dependence of the wavelength tuning rate  $d\lambda/dT$  is  $\sim 0.5$  nm/ $^\circ\text{C}$  from 45  $^\circ\text{C}$  to 180  $^\circ\text{C}$ , which permits us to have the widely tunable range of SHG. Furthermore, the wide temperature bandwidth of  $\Delta T = 14.8$   $^\circ\text{C}$  and angle bandwidth of  $\Delta\theta = 4.24$   $^\circ$  at 25  $^\circ\text{C}$  will reveal unique performance in the SHG applications. With these advantages, we believe that type II broadband SHG in PPKTP may have potential applications in the efficient broadband SHG and other nonlinear optical frequency conversion processes.

This research was supported by the National Natural Science Foundation of China (grants 60407006 and 60477016) and the Foundation for Development of Science and Technology of Shanghai (grant 04DZ14001).

### References

1. N. E. Yu, J. H. Ro, M. Cha, S. Kurimura, and T. Taira, "Broadband quasi-phase-matched second-harmonic generation in MgO-doped periodically poled LiNbO<sub>3</sub> at the communications band," *Opt. Lett.* **27**, 1046–1048 (2002).
2. N. E. Yu, S. Kurimura, K. Kitamura, J. H. Ro, M. Cha, S. Ashihara, T. Shimura, K. Kuroda, and T. Taira, "Efficient frequency doubling of a femtosecond pulse with simultaneous group-velocity matching and quasi phase matching in periodically poled, MgO-doped lithium niobate," *Appl. Phys. Lett.* **82**, 3388–3390 (2003).
3. S. Wang, V. Pasiskevicius, J. Hellstrom, F. Laurell, and H. Karlsson, "First-order type II quasi-phase-matched UV generation in periodically poled KTP," *Opt. Lett.* **24**, 978–980 (1999).
4. V. Pasiskevicius, S. J. Holmgren, S. Wang, and F. Laurell, "Simultaneous second-harmonic generation with two orthogonal polarization states in periodically poled KTP," *Opt. Lett.* **27**, 1628–1630 (2002).
5. T. A. Driscoll, H. J. Hoffman, R. E. Stone, and P. E. Perkins, "Efficient second-harmonic generation in KTP crystals," *J. Opt. Soc. Am. B* **3**, 683–686 (1986).
6. B. Boulanger, J. P. Feve, G. Marnier, C. Bonnin, and P. Villeval, "Absolute measurement of quadratic nonlinearities from phase-matched second-harmonic generation in a single KTP crystal cut as a sphere," *J. Opt. Soc. Am. B* **14**, 1380–1386 (1997).
7. A. Arie, G. Rosenman, V. Mahal, A. Skliar, M. Oron, M. Katz, and D. Eger, "Green and ultraviolet quasi-phase-matched second harmonic generation in bulk periodically-poled KTiOPO<sub>4</sub>," *Opt. Commun.* **142**, 265–268 (1997).
8. K. Tradkin, A. Arie, A. Skliar, and G. Rosenman, "Tunable mid-infrared source by difference frequency generation in bulk periodically poled KTiOPO<sub>4</sub>," *Appl. Phys. Lett.* **74**, 914–916 (1999).
9. V. Pasiskevicius, S. Wang, J. A. Tellefsen, F. Laurell, and H. Karlsson, "Efficient Nd:YAG laser frequency doubling with periodically poled KTP," *Appl. Opt.* **37**, 7116–7119 (1998).
10. CASIX, <http://www.casix.com> (2003).
11. M. M. Fejer, G. A. Magel, D. H. Jundt, and R. L. Byer, "Quasi-phase-matched second harmonic generation: tuning and tolerances," *IEEE J. Quantum Electron.* **28**, 2631–2654 (1992).
12. H. Ishizuki, I. Shoji, and T. Taira, "Periodical poling characteristics of congruent MgO:LiNbO<sub>3</sub> crystals," *Appl. Phys. Lett.* **82**, 4062–4063 (2003).